Braz J Phys (2013) 43:214–222
DOI 10.1007/s13538-013-0134-1

CONDENSED MATTER

Cluster Method Calculation of the Curie Temperature and Exchange Parameters for the Magnetocaloric Compounds $MnFeAs_xP_{1-x}$ ($0.25 \leq x \leq 0.65$) and Hexagonal MnFeAs

Osvaldo F. Schilling

Received: 27 October 2012 / Published online: 31 May 2013

Abstract A wealth of experimental and theoretical data on the crystallographic and magnetic properties of the magnetocaloric compounds $MnFeAs_xP_{1-x}$ ($0.25 \leq x \leq 0.65$) and MnFeAs has become available in the last decade. By analyzing the data and treating the spin interactions with Callen's cluster expansion method, we extrapolate first-principle results for the exchange-coupling constants of MnFeAs to the P-substituted compounds and find Curie temperatures that agree, within 5 % deviation, with experiment. Simulations with different coupling parameters show that T_c is weakly dependent on the Fe–Fe interactions. Analysis of lattice expansion as a function of composition shows that changes in the lattice parameters a and c have opposite effects upon the strength of the magnetic interactions between ions. The results indicate that the cluster expansion method provides reliable estimates of magnetic properties, even for metallic compounds characterized by multiple interactions among ions with distinct magnetic moments.

Keywords Magnetocaloric effect · Cluster methods · Constant coupling approximation · Heisenberg model

PACS 75.30.Sg · 75.10.Jm · 75.30.Kz

1 Introduction

The simulation of physical properties of materials has acquired increasing importance in view of the improved synthesis techniques developed in recent years. Such theoretical studies provide helpful guidance to the experimentalist or materials scientist in search of optimized compositions to try or of novel properties to measure and explore. In particular, the development of materials for magnetic refrigeration has motivated a series of papers dedicated to the simulation and phenomenological description of their thermomagnetic properties [1–3]. In the present paper, we shall concentrate on materials of this kind and their magnetic properties.

1.1 Cluster Methods

The central theoretical tool in the analysis of magnetic systems is the Heisenberg Hamiltonian, either on its own or accompanied by kinetic and interaction energy terms describing itinerant electrons in an enlarged Hamiltonian. In the 1950s and 1960s, methods were developed to obtain approximate solutions for the Heisenberg model of interacting localized magnetic moments [4]. The high-temperature expansion (HTE) method [5] provides accurate calculations of critical temperatures for different spin lattices and sets benchmarks against which approximate calculation methods have been compared. The assumption of localized spins, usually made in the study of most materials, is justified even for metals, since the itinerant electrons in transition metal alloys and compounds only constitute a small fraction of the d-electrons [6, 7]. With the advance of computational techniques, detailed density functional calculations have recently been carried out to associate band-structure and density-of-state data for conduction electrons with the exchange interactions in the Heisenberg Hamiltonian [8, 9], a development from which the present study benefits, as discussed below. Important as density-functional calculations are, however, first-principle methods have not been applied to the computation of such important properties as the temperature or magnetic field dependence of magnetization, correlation functions, and entropy, in view of the complexity of the required methods.

O. F. Schilling (✉)
Departamento de Física, Universidade Federal de Santa Catarina, Campus, Trindade, 88040-900, Florianópolis, Santa Catarina, Brazil
e-mail: osvaldo.neto@ufsc.br

A good compromise between simplicity and accuracy in the theoretical treatment of interactions between magnetic moments is offered by the cluster mean-field models. Central in this approach is a cluster with a small number of spins. The interactions within the cluster are precisely accounted for, while the effect of the remaining spins in the system upon the cluster spins is represented by an average mean field. The earliest such cluster-based theory is Pierre Weiss's molecular-field theory (MFT) [4]. In the MFT, the cluster comprises a single spin, subject to an averaged field from all other spins. The MFT is popular because it is both simple and able to numerically fit most measurable thermodynamic and magnetic properties of a given distribution of magnetic moments, provided that a sufficiently large number of fitting parameters be adjusted. It is widely used to fit measured properties of such technologically important materials as rare-earth iron garnets and boracites, for instance, whose multiple-sublattice structure challenges more detailed treatment. However, since it is unable to account for the correlations between spins, the MFT makes only qualitatively accurate predictions. A few examples suffice to identify the weaknesses of Weiss's method. Although it predicts ferromagnetic (FM) and antiferromagnetic phase transitions, the MFT yields critical temperatures that are too high for a given exchange parameter and subsist independently of the spin lattice geometry, a result proven incorrect by all more precise methods. The MFT incorrectly predicts the specific heat to vanish above the transition and has no provision for spin waves at low temperatures. The computation of reliable critical exponents lies outside the scope of the procedure. Although the quality of its predictions grows with the magnetic moments of the ions and with the density of the structures [4], the MFT is inappropriate for the purposes of the present study, which proposes to derive a set of exchange constants for magnetocaloric materials in consistency with the measured Curie temperatures T_c, because MFT is unable to correctly predict T_c.

The deficiencies of the single-spin cluster treatment are alleviated when the cluster size is increased. The earliest such models is the Bethe–Peierls–Weiss (BPW) cluster model, which treats the interaction between a central spin and the layer of nearest neighbors (nn) precisely, while the nn layer is subject to an effective field representing the rest of the lattice [4]. Improved results are obtained for T_c, the spin correlations, etc., but the BPW theory incorrectly predicts the magnetization to drop to zero at low temperatures in the ferromagnetic state—the so-called anti-Curie point. The theory is therefore only applicable close to the transition and at higher temperatures.

In the mid-1950s, the work of Kastelejn and van Kranendonk (KvK) and of Oguchi [4] showed that a cluster of two or three spins constitutes a very good compromise between accuracy and simplicity, at least above $T_c/2$ and hence in the temperature range of interest for applications of the magnetocaloric materials. The cluster method of KvK is called the constant-coupling method because it assumes that the exchange parameter J between the pair of spins forming the cluster is temperature-independent, an assumption that is appropriate at high temperatures. The distinctive feature of the KvK method, which makes it conceptually superior to Oguchi's pair-cluster approach and to the BPW method, is the consistency in the minimization criterion that yields the average magnetization, based on proper minimization of the total system free energy [10, 11]. Initially restricted to $S=1/2$ and to spin pairs in isotropic Heisenberg Hamiltonians, the KvK method was extended by Strieb et al. and Callen and Callen [10, 11] to higher spins and separation-dependent exchange constants. To impose the consistency criterion, Callen and Callen minimize the overall free energy along a proper expansion of the spin lattice in increasingly larger clusters that starts with isolated spins—the Callen cluster expansion method [10, 11]. Here, we adopt this approach. We will expand the free energy in the Callen–Callen style, accounting for both single-spin and spin-pair clusters, also allowing for next-nearest-neighbor interactions.

1.2 Application to $MnFeAs_xP_{1-x}$ ($0.25 \le x \le 0.65$) and Hexagonal MnFeAs

We apply the cluster expansion method to the paramagnetic (PM)–ferromagnetic transitions of a series of structurally related compounds, $MnFeAs_xP_{1-x}$ ($0.25 \le x \le 0.65$) and hexagonal FeMnAs, with a view to finding exchange coupling constants compatible with the experimental T_c for all compositions. We choose these materials because their important magnetocaloric properties have raised much interest. Our analysis benefits from the linear muffin-tin orbital first-principle computations of the exchange coupling constants for the hexagonal-phase compound FeMnAs by Liu and Altounian [12].

FeMnAs crystallizes in the hexagonal Fe_2P form under high-pressure–high-temperature conditions, the reported T_c being close to 190 K [13]. Substitution of P, Ge, or Si for As pushes the Curie temperature up to 300 K or more [14, 15]. We give particular attention to results in [16, 17], which applied neutron diffraction to the $MnFeAs_xP_{1-x}$ ($0.25 \le x \le 0.65$) compounds to investigate their magnetic transitions.

Given the reported exchange constants [12], we have developed a model to calculate T_c. The procedure was first tested on FeMnAs and subsequently applied to the other P-substituted compounds. We have applied the cluster expansion method to the five sets of nearest-neighbor and next-nearest-neighbor pairs reported in [12], chosen according to the strength of the interactions.

To estimate the exchange couplings for $MnFeAs_xP_{1-x}$, we have relied on an extrapolation procedure. Since the lattice constants of $MnFeAs_xP_{1-x}$ are known for several

compositions in the range $0.25 \leq x \leq 0.65$ [16], we have associated those constants with the T_c data in [17] to construct an expression that extrapolates from the data in [12] to yield the exchange coupling constants as functions of the composition. We have then applied the cluster expansion method to calculate T_c for each composition in [17] and checked that the computed critical temperatures compare favorably with the experimental values reported in that paper.

In the remainder of this paper, the following sequence of exposition is adopted. In Section 2, the theoretical model for the calculation of T_c is detailed. In Section 3, the Curie temperature is calculated for MnFeAs from the exchange constants in [12] by means of the cluster expansion method. The crystallographic data for the compounds in [16] are next analyzed and associated to the magnetic measurements in [17]. The data are then correlated to yield expressions for the main exchange constants as functions of the composition, with the constants for MnFeAs as input. The Curie temperatures are then obtained for all compounds $MnFeAs_xP_{1-x}$ and compared with experiment [17] to check the consistency of the calculated exchange constants. Finally, Section 4 collects our conclusions.

2 Cluster Expansion Model of the Magnetism of Hexagonal FeMnAs

Figure 1 shows the most important details of the unit cell of FeMnAs in its hexagonal form. The metal ions are distributed in parallel alternating planes separated by half the unit-cell parameter c, with As atoms (not shown) separating neighbors on the same plane. The Fe and Mn atoms, which are located in different environments coordinated by the As atoms, are magnetically quite different [12, 13]. As indicated by the atomic coordinates listed in [12], the geometrical orientation of the neighbors around each magnetic ion in this basis is a slightly irregular hexagon. In our model, however, each metal has six equivalent nn metal atoms hexagonally distributed on the basal plane and additional six Fe or Mn neighbors on the planes just above or below them. The number of nnn around each metallic atom is also assumed to be six, all located on their own planes.

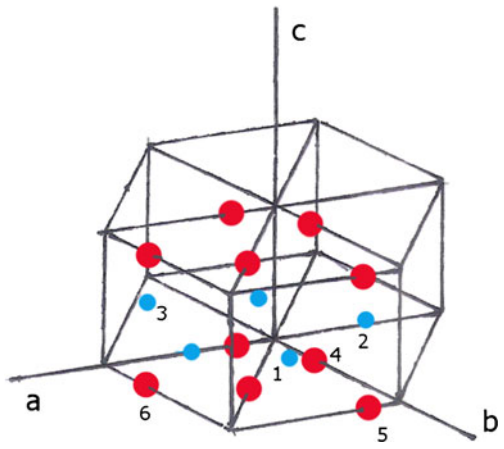

Fig. 1 (Colored online) Unit cell of hexagonal FeMnAs. The larger, *red circles* represent the Fe atoms; the smaller, *blue* ones represent the Mn atoms; the As atoms are not shown. The numbers are used to identify the pairs of spins, which are described in the text

Liu and Altounian and Tobola et al. [12, 13] have obtained 3.1 μ_B and 1.1 μ_B for the magnetic moments of Mn and Fe, in fair agreement with the experimental values of 3.1 μ_B and 1.5 μ_B, respectively. The total per-formula calculated moment is 4.2 μ_B, also close to the experimentally observed 4.5 μ_B. In view of these results, we describe the Mn and Fe atoms in our model by spins 3/2 and 1/2, respectively, with g factors of 2. Liu and Altounian [12] have determined the exchange constants for a Heisenberg Hamiltonian describing this compound. The most important results, taken from Fig. 6 in [12], are collected in Table 1, which includes all the interatomic couplings down to at least 25 % of the nn coupling for each Fe–Fe, Mn–Fe, and Mn–Mn pair. For simplicity, we neglect the remaining weak interactions between more distant neighbors and are left with five relevant spin-pair couplings.

We refer to the labels in Fig. 1 to identify the five types of spin pairs in our calculations. Two pairs lie on each Mn (pairs 1–2 and 1–3) and Fe planes (pairs 4–5 and 4–6). Another pair couples two nn ions, a Mn atom and an Fe atom, on different planes (pair 1–4). In our notation, J_{11} and J_{12} are the exchange interactions in the Mn plane between the nn 1–2 and nnn 1–3 atoms, respectively. J_{21} and J_{22} are the corresponding constants in the Fe plane for atoms 4–5 and 4–6, and K is the exchange interaction between nn Fe (4) and Mn (1) atoms.

The cluster expansion method of Strieb et al. and Callen and Callen [10, 11] expands the free energy for the full-spin system into a sum of energy terms, starting with isolated spins and continuing with progressively more complex clusters. In our model, the most complex clusters are the spin pairs. The five types of spin pairs are taken as statistically independent. The free energy will therefore be obtained

Table 1 Exchange coupling parameters for MnFeAs from [12]

Ions	d	Notation	Coupling parameters (K)
Mn–Mn (nn)	0.5	$2J_{11}$	60
Mn–Mn (nnn)	1	$2J_{12}$	28
Fe–Fe (nn)	0.45	$2J_{21}$	−70
Fe–Fe (nnn)	0.65	$2J_{22}$	−23
Mn–Fe(nn)	0.43	$2K$	104

In [12], 1mRy=157.7 K. Interatomic distances d are in fractions of the lattice parameter a

from the logarithm of the product of the pair partition functions, that is, from the sum of the logarithms of the partition functions. Each pair partition function is computed from the trace of the corresponding density operator. We work with five density operators for the spin pairs *i*–*j*, which depend on the corresponding Hamiltonian operators $H_{i\ j}$. In the notation of Fig. 1, the latter are described by the expressions

$$H_{12}(\mathrm{Mn{-}Mn}) = -2\ J_{11}\mathbf{S}_1{\cdot}\mathbf{S}_2 - 2H_{\mathrm{Mn},h,1}\left(S_{z,1}+S_{z,2}\right) \quad (1)$$

$$H_{13}(\mathrm{Mn{-}Mn}) = -2J_{12}\mathbf{S}_1{\cdot}\mathbf{S}_3 - 2H_{\mathrm{Mn},h,2}\left(S_{z,1}+S_{z,3}\right) \quad (2)$$

$$H_{14}(\mathrm{Mn{-}Fe}) = -2\ K\ \mathbf{S}_1{\cdot}\mathbf{S}_4 - 2H_{\mathrm{Mn},v}\left(S_{z,1}+S_{z,4}\right) + 2\,\Delta H\,S_{z,4} \quad (3)$$

$$H_{45}(\mathrm{Fe{-}Fe}) = -2\ J_{21}\ \mathbf{S}_4{\cdot}\mathbf{S}_5 - 2H_{\mathrm{Fe},h,1}\left(S_{z,4}+S_{z,5}\right) \quad (4)$$

$$H_{46}(\mathrm{Fe{-}Fe}) = -2\ J_{22}\ \mathbf{S}_4{\cdot}\mathbf{S}_6 - 2H_{\mathrm{Fe},h,2}\left(S_{z,4}+S_{z,6}\right) \quad (5)$$

In Eqs. (1)–(5), $\Delta H = H_{\mathrm{Mn},v} - H_{\mathrm{Fe},v}$, with $H_{\mathrm{Mn},v}=(6\ J_{11}+6\ J_{12}+5K)h_1$, $H_{\mathrm{Fe},v}=(6\ J_{21}+6\ J_{22}+5K)h_2$, $H_{\mathrm{Mn},h,1}=(5\ J_{11}+6\ J_{12}+6K)h_1$, $H_{\mathrm{Mn},h,2}=(6\ J_{11}+5\ J_{12}+6K)h_1$, $H_{\mathrm{Fe},h,1}=(5\ J_{21}+6\ J_{22}+6K)h_2$, $H_{\mathrm{Fe},h,2}=(6\ J_{21}+5\ J_{22}+6K)h_2$, where h_1 and h_2 are the effective fields per neighboring spin acting on each Mn or Fe atom, respectively, in the absence of external magnetic fields.

Equations (1)–(5) rigorously account for the in-pair interactions and treat the remaining interactions via the aforementioned effective fields $H_{\mathrm{Mn},v}$, $H_{\mathrm{Fe},v}$,…, $H_{\mathrm{Fe},\ h,2}$. The subscripts *h* and *v* denote intra-plane and inter-plane interactions, respectively. The effective fields are determined by minimization of the overall free energy, which leads to the consistency condition detailed in [10, 11]. We are here concerned with PM–FM transitions, which correspond to positive h_1 and h_2. Nonetheless we note that, since the metal ions are disposed in intercalated layers, the model might exhibit solutions with h_1 and h_2 of opposite signs, that is, antiferromagnetic solutions.

To derive the consistency conditions determining h_1 and h_2, we have to write down the cluster expansion expression for the free energy of the spin system. For an expansion limited to clusters of spin pairs, the free energy *F* has the form [10, 11]

$$-\beta F = -(3z-1)N\ln\left(\mathrm{Tr}_i\rho_{\mathrm{Mn},i}\right) - (3z-1)N\ln\left(\mathrm{Tr}_i\rho_{\mathrm{Fe},i}\right) + Nz\ln(\mathrm{Tr}_1\mathrm{Tr}_4\rho_{14}) + Nz/2\ln(\mathrm{Tr}_1\mathrm{Tr}_2\rho_{12}) + \ldots\ldots + Nz/2\ln(\mathrm{Tr}_4\mathrm{Tr}_6\rho_{46}) \quad (6)$$

where *N* is the number of metal atoms of each type, Fe or Mn; $z=6$ is the number of intra- and inter-plane nn and also the number of nnn in the planes, $\beta=1/T$; and Tr denotes the trace operation.

Equation (6) displays the structure of the free-energy expansion in progressively more complex cluster terms. Therefore, the first two terms on the right-hand side of Eq. (6) are the free energies calculated for isolated (*i*) Mn and Fe ions, whose Hamiltonians are simply

$$H_i(\mathrm{Mn}) = -2H_{\mathrm{Mn},i}S_{z,\mathrm{Mn}} \quad (7)$$

and

$$H_i(\mathrm{Fe}) = -2H_{\mathrm{Fe},i}S_{z,\mathrm{Fe}}, \quad (8)$$

where $H_{\mathrm{Mn},i}=6(K+J_{11}+J_{12})h_1$ and $H_{\mathrm{Fe},i}=6(K+J_{21}+J_{22})h_2$ are the isolated-ion effective fields. In Eq. (6), each density matrix ρ is defined as $\exp(-\beta H)$ divided by the partition function, for the Hamiltonian operators in Eqs. (1)–(5) and (7)–(8).

We calculate the eigenvalues of the five Hamiltonians (1)–(5), on the basis of eigenfunctions of $\mathbf{S}_k^2, \mathbf{S}_l^2, \mathbf{R}^2_{kl}=(\mathbf{S}_k+\mathbf{S}_l)^2$ and $M_{kl}=S_{z,k}+S_{z,l}$ (for each *k*–*l* pair) and from them build the corresponding partition functions Z_{kl}. Next, to compute the averages of the *z*-components of the ion magnetizations $\langle S_z\rangle_{kl}$ for each Hamiltonian, we compute the derivative of $\ln(Z_{kl})$ with respect to H_{Fe} or H_{Mn}. This corresponds to carrying out the double traces in Eq. (6) and calculating the derivative. The results are equivalent to those obtained by the constant-coupling method (see for instance [4, 18]), except for Eq. (3). In this case, since $S_{z,4}$ does not commute with $\mathbf{R}^2_{14}$, the Hamiltonian has off-diagonal terms given by Clebsch–Gordan coefficients, and the eigenvalues are obtained by the methods applied in the analysis of the Zeeman effect [19] or the Bethe–Peierls–Weiss model [20].

We only present the most important details of the calculations. In particular, we obtain the eigenvalues of the Hamiltonian in Eq. (1). The same method can be applied to Eqs. (2), (4), and (5). In Eq. (1) the operator $\mathbf{S}_1\ \mathbf{S}_2$ is given by the following well-known relation:

$$2\ \mathbf{S}_1{\cdot}\mathbf{S}_2 = (\mathbf{S}_1+\mathbf{S}_2)^2 - \mathbf{S}_1{}^2 - \mathbf{S}_2{}^2 = \mathbf{R}_{12}{}^2 - \mathbf{S}_1{}^2 - \mathbf{S}_2{}^2 \quad (9)$$

The eigenstates of $\mathbf{R}_{12}{}^2$, $\mathbf{S}_1{}^2$, and $\mathbf{S}_2{}^2$ therefore diagonalize the Hamiltonian (1). From Eq. (9), we obtain the eigenvalues of $2\mathbf{S}_1\ \mathbf{S}_2$, which are $r(r+1)-2s_{\mathrm{Mn}}(s_{\mathrm{Mn}}+1)$, where $s_{\mathrm{Mn}}=3/2$ and *r* can take the integer values between $2s_{\mathrm{Mn}}$ and zero. The second part of the Hamiltonian for this nn Mn pair contains an effective field term multiplied by the total *z* component of the magnetic moment operator M_{12} for the pair 1–2. The eigenvalues of M_{12} are proportional to *m*, the total *z*-component of the moment for this pair, which runs between $-r$ and *r* in unit steps, for each *r*. Therefore, the

energies associated with the Hamiltonian (1) are given by the equality

$$\varepsilon_{12}(r,m) = -J_{11}r(r+1) - 2H_{\mathrm{Mn},,h,,1}\ m \tag{10}$$

with r=0, 1, 2, and 3 and m=− r, …, r. We have neglected a constant term, which simply shifts the energy zero. The resulting partition function is [4]:

$$Z_{12}\left(J_{11}, H_{\mathrm{Mn},,h,,1}, \beta\right) = \sum_{m=-r}^{r}\sum_{r=0}^{3}\exp\left\{\beta\left(J_{11}\,r(r+1) + 2\ H_{\mathrm{Mn},,h,,1}\ m\right)\right\} \tag{11}$$

Differentiation of Eq. (11) with respect to $H_{\mathrm{Mn},,h,,1}$ yields the following expression for the average moment for each Mn ion in the pair 1–2:

$$< S_{z,\mathrm{Mn}} >_{12} = \frac{1}{2\beta Z_{12}}\frac{\partial Z_{12}}{\partial H_{\mathrm{Mn},,h,,1}} \tag{12}$$

As explained earlier, application of the same procedure to the Mn–Mn pair 1–3 and to the Fe–Fe pairs 4–5 and 4–6 (with s_{Fe}=1/2), respectively, yields $<S_{z,\ \mathrm{Mn}}>_{13}$, $<S_{z,\ \mathrm{Fe}}>_{45}$, and $<S_{z,\ \mathrm{Fe}}>_{46}$.

The Hamiltonian (3), which describes the inter-plane interaction between neighboring Mn and Fe ions 1 and 4, deserves special attention since the $S_{z,4}$ operator in the last term on the right-hand side does not commute with $\mathbf{R}_{14}{}^2$. Therefore, the eigenstates of this Hamiltonian are linear combinations of the eigenstates of $\mathbf{S}_1{}^2$, $\mathbf{S}_4{}^2$, $\mathbf{R}^2{}_{14}$, and M_{14} =$S_{z,1}$+$S_{z,4}$, with coefficients given by the Clebsch–Gordan coefficients. From the addition of the Mn spin 3/2 with the Fe spin 1/2 one obtains the following set of eigenstates | r, m>: | 2, 2 >, |2, −2>, | 2, 1>,| 2, −1>, | 2,0>, | 1,1>, | 1,0>, and | 1, −1>. The operator $S_{z,4}$ couples the states according to the following rules (in units of $\hbar$) [19, 20]:

$$< 3/2 \pm 1/2, m \left| S_{z,4} \right| 3/2 \pm 1/2, m >= \pm m/4 \tag{13}$$

$$< 3/2 \pm 1/2, m \left| S_{z,4} \right| 3/2 \mp 1/2, m = -\frac{1}{4}\sqrt{4-m^2} \tag{14}$$

Clearly, the pairs of states | 2, 1> and | 1, 1>; | 2, 0> and | 1, 0>; and | 2, −1>and | 1, −1> are coupled to each other, while the states | 2,2>and |2, −2> are fully decoupled. To obtain the full set of eigenstates of $S_{z,4}$, we therefore have to diagonalize three 2×2 matrices, whose elements are given by the coefficients in Eqs. (13) and (14). To obtain the matrix elements, we simply operate on both sides of the Hamiltonian with the corresponding state vectors for each pair of states. The following energies result:

$$\varepsilon_{14}\left(|\,2,2>\right) = -3K - 4\ H_{\mathrm{Mn},v} + \Delta H \tag{15}$$

$$\varepsilon_{14}\left(|\,2,-2\right) = -3K + 4\ H_{\mathrm{Mn},v} - \Delta H \tag{16}$$

$$\varepsilon_{14}(\,|2,1>;|1,1>)_{\pm} = K - 2\ H_{\mathrm{Mn},v} \pm \sqrt{16K^2 - 4K\Delta H + (\Delta H)^2} \tag{17}$$

$$\varepsilon_{14}(\,|2,-1>;|1,-1>)_{\pm} = K + 2\ H_{\mathrm{Mn},v} \pm \sqrt{16K^2 + 4K\Delta H + (\Delta H)^2} \tag{18}$$

$$\varepsilon_{14}(\,|2,0>;|1,0>)_{\pm} = K \pm \sqrt{16K^2 + (\Delta H)^2} \tag{19}$$

Given these eight energies, we follow a procedure analogous to the one leading to Eq. (12) and construct the partition function Z_{14}. The average values for the moments of the Fe and Mn ions in the pair are:

$$< S_{z,\mathrm{Fe}} >_{14} == \frac{1}{\beta Z_{14}}\frac{\partial Z_{14}}{\partial H_{\mathrm{Fe},\,v}} \tag{20}$$

$$< S_{z,\mathrm{Mn}} >_{14} = \frac{1}{\beta Z_{14}}\frac{\partial Z_{14}}{\partial H_{\mathrm{Mn},\,v}} \tag{21}$$

The final step in the analysis is the determination of the averaged magnetization for the isolated ions, $<S_{z,\mathrm{Mn}}>_i$ and $<S_{z,\mathrm{Fe}}>_i$, which reduce to Brillouin functions of the pertinent spins, 1/2 for Fe or 3/2 for Mn [4].

To find the effective fields h_1 and h_2, we minimize Eq. (6) with respect to h_1 and h_2. In practice, when partial derivatives are evaluated with respect to the effective fields, the average magnetizations appear on the right-hand side of Eq. (6). The following pair of equations results, to be numerically solved:

$$\begin{aligned} 17(K + J_{11} + J_{12})\langle\, S_{z,\mathrm{Mn}}\,\rangle_i &= (5J_{11} + 6J_{12} + 6K)\langle\, S_{z,\mathrm{Mn}}\,\rangle_{12} \\ &+ (6J_{11} + 5J_{12} + 6K)\langle\, S_{z,\mathrm{Mn}}\,\rangle_{13} \\ &+ (6J_{11} + 6J_{12} + 5K)\langle\, S_{z,\mathrm{Mn}}\,\rangle_{14} \end{aligned} \tag{22}$$

$$\begin{aligned} 17(K + J_{21} + J_{22})\langle S_{z,\mathrm{Fe}}\rangle_i &= (5J_{21} + 6J_{22} + 6K)\langle\, S_{z,\mathrm{Fe}}\,\rangle_{45} \\ &+ (6J_{21} + 5J_{22} + 6K)\langle S_{z,\mathrm{Fe}_{46}}\rangle \\ &+ (6J_{21} + 6J_{22} + 5K)\langle S_{z,\mathrm{Fe}}\rangle_{14} \end{aligned} \tag{23}$$

Equations (22) and (23) are the central results of this work. Our search for the per-neighbor effective fields h_1

and h_2 has determined the temperature dependence of the magnetization at zero external magnetic field. We will restrict our investigation to the limit of vanishing effective fields, to find the Curie temperature. In this limit, Eqs. (22) and (23) become linear in h_1 and h_2 and can be written in the forms

$$a(1,1)h_1 + a(1,2)h_2 = 0 \tag{22a}$$

$$a(2,1)h_1 + a(2,2)h_2 = 0 \tag{23a}$$

where:

$$a(1,1) = 85(1+\varepsilon+\gamma)^2 - (5+6\gamma+6\varepsilon)^2\left(28/a^6 + 10/a^3 + 2/a\right)/\left(12/a^6 + 10/a^3 + 6/a + 2\right) - (6+6\gamma+5\varepsilon)^2\left(28/d^6 + 10/d^3 + 2/d\right)/\left(12/d^6 + 10/d^3 + 6/d + 2\right) - (6+5\gamma+6\varepsilon)^2\left(b^2 + 1/b^2 - \left(1/2 - 3(8\ln b)\right)\left(b^2 - 1/b^2\right)/\left(3\left(b^2 + 1/b^2\right)\right)\right) \tag{24}$$

$$a(1,2) = -(6\delta+5\gamma+6\eta)(6+5\gamma+6\varepsilon)\left(3/(8\ln b)\right)\left(b^2 - 1/b^2\right)/\left(3\left(b^2 + 1/b^2\right)\right) \tag{25}$$

$$a(2,1) = (6\delta+5\gamma+6\eta)(6+5\gamma+6\varepsilon)\left(1/2 - 3/(8\ln b)\right)\left(b^2 - 1/b^2\right)/\left(3\left(b^2 + 1/b^2\right)\right) \tag{26}$$

$$a(2,2) = 51(\delta+\varepsilon+\gamma)^2 - (5\delta+6\gamma+6\varepsilon)^2\left(1/c\right)/\left(1 + 3/c\right) - (6\delta+6\gamma+5\varepsilon)^2\left(1/e\right)/\left(1 + 3/e\right) - (6\delta+5\gamma+6\eta)^2\left(3/(8\ln b)\right)\left(b^2 - 1/b^2\right)/\left(3\left(b^2 + 1/b^2\right)\right) \tag{27}$$

Here we have divided all the exchange constants in Eqs. (22) and (23) by J_{11} so that γ, δ, ε, and η represent K/J_{11}, J_{21}/J_{11}, J_{12}/J_{11}, and J_{22}/J_{11}, respectively. We have also introduced the shorthands $a=\exp(2\beta J_{11})$, $b=\exp(2\beta K)$, $c=\exp(2\beta J_{21})$, $d=\exp(2\beta J_{12})$, and $e=\exp(2\beta J_{22})$.

The Curie temperature is given by the higher-temperature root of the determinant

$$\Delta = a(1,1)a(2,2) - a(1,2)a(2,1) \tag{28}$$

Substitution of the exchange parameters into Eq. (28) leads to roots that will be discussed in Section 3.

3 Magnetic and Crystallographic Properties and Their Relationship

3.1 Determination of T_c for MnFeAs

Given a set of exchange parameters, the roots of Eq. (28) can be easily obtained, numerically. A more convenient way to discuss the parametrical dependence of the Curie temperature is to plot the logarithm of the absolute value of Δ as a function of the temperature. The exponential functions a, b, c, d, and e make (the absolute value of) Δ vary by several orders of magnitude as a function of temperature even in a small interval close to the Curie temperature. The logarithmic plot clearly identifies T_c at the junction of two sharp cusps.

Before comparing with experiment, one must analyze the PM–FM transition data on MnFeAs by Tobola et al. [13]. Figure 4 of [13] displays the thermal dependence of the magnetization under a field of 0.1 T, which indicates a T_c close to 190 K. Insertion of the numbers from Table 1, that is, $2J_{11}$=60 K, $2J_{12}$=28 K, $2J_{21}$=−70 K, $2J_{22}$=−23 K, and $2K$=104 K, into Eq. (28), yields the root of Δ at T_c=206 K. The cluster expansion method is therefore capable of predicting T_c with 8 % accuracy.

It is by now well established that the exchange couplings can be tuned by partial substitution of smaller ions, such as P, for As, so that T_c rise to room temperature and above [14, 15, 17]. This indicates that T_c is a strong function of the interactions within the higher-spin Mn planes, with some contribution from the Fe-plane interactions. In order to examine such possibilities, we carried out additional simulations with MnFeAs, changing the nn exchange parameter in the Fe planes only. Figure 2 displays simulations

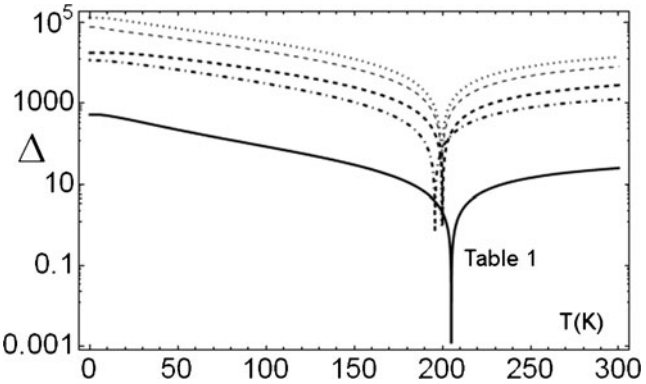

Fig. 2 Logarithm of the absolute value of Δ as a function of temperature for different Fe–Fe intra-plane interactions J_{21}. From top, $2J_{21}(K)$ =50, 20, −20, −120, and −70 The lowest plot, represented by a *bold solid line*, is based on the numbers in Table 1, from [12]. The Curie temperature T_c≈190–200 K is largely insensitive to the changes in J_{21}

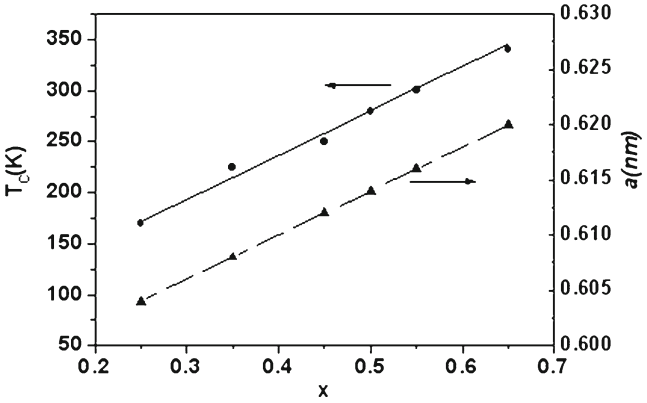

Fig. 3 Experimental results for the dependences of T_c [17] and the basal-plane lattice constant [16] on x in $MnFeAs_xP_{1-x}$ ($0.25 \le x \le 0.65$)

involving large changes in J_{21}, from positive to negative values, while keeping the other parameters unchanged. We plot logΔ as a function of T for different J_{21}'s. The solid curve is the one resulting from Liu and Altounian's data for MnFeAs, with its pair of cusps pointing straight down to the root at 206 K. The Curie temperature is essentially independent of J_{21}. Even when the exchange coupling turns positive, T_c remains close to 200 K. This clear evidence that the couplings within the Fe plane have little effect on the PM–FM transition is an important result, rather easily obtained from the cluster method.

3.2 Relation Between the Composition and T_c, the Lattice Expansion, and the Exchange Parameters

Figure 3 shows experimental data for T_c [17] and the basal plane lattice constant a [16] as functions of the composition x in $MnFeAs_xP_{1-x}$ ($0.25 \le x \le 0.65$), in the PM state. By comparison, the lattice constant c remains comparatively unaltered at $c=0.3486 \pm 0.0002$ nm over the entire composition range. Given the good correlation with the behavior of T_c, we conclude that the electronic overlap along the basal planes, modulated by the effect of P substitution upon the lattice parameter, controls the exchange constants of the P-substituted compounds. Along the series, T_c is linearly

Table 2 Exchange coupling parameters (in kelvin) for $MnFeP_{1-x}As_x$ from Eq. (29) and Table 1

x	$2J_{11}$	$2J_{12}$	$-2J_{21}$	$-2J_{22}$	$2K$
0.25	56	26	66	22	97
0.35	69	32	81	27	120
0.45	82	38	96	32	142
0.50	88	41	103	34	153
0.55	94	44	110	36	164
0.65	104	50	125	41	186

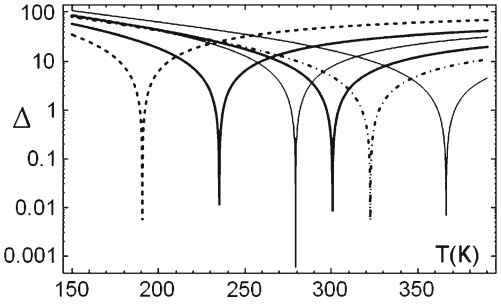

Fig. 4 Logarithm of the absolute value of Δ, calculated from the parameters in Table 2, as a function of the temperature for $x=0.25$, 0.35, 0.45, 0.5, 0.55, and 0.65 in $MnFeAs_xP_{1-x}$, from *left* to *right*. Each cusp indicates the Curie temperature for the corresponding compound

related to the expansion ratio $\delta a/a_0$ where $a_0=a(x=0.5)$, with $\delta a=a(x)-a_0=a(x)-0.614$ nm.

Consider now the parent compound MnFeAs. Albeit larger than the parameters represented by the solid triangles in Fig. 3, the lattice parameter $a=0.6249$ nm of MnFeAs is somewhat smaller than the extrapolation of the dashed line in Fig. 3 to $x=1$. By contrast, the Curie temperatures and the lattice parameters c for the parent compound and the P-substituted compounds are very different. The Curie temperature $T_c \approx 190$ K for the parent compound lies hundreds of degrees below the extrapolation of the solid line to $x=1$. The parameter $c=0.360$ nm is substantially larger than the parameters for $0.25 \le x \le 0.65$. This indicates that the relatively low T_c in the parent compound is due to the expanded c parameter. We conclude that the dependence of the exchange couplings on expansions parallel to the basal plane is distinct from the dependence on expansions normal to that plane and combine our conclusion with the available crystallographic data to write a phenomenological expression

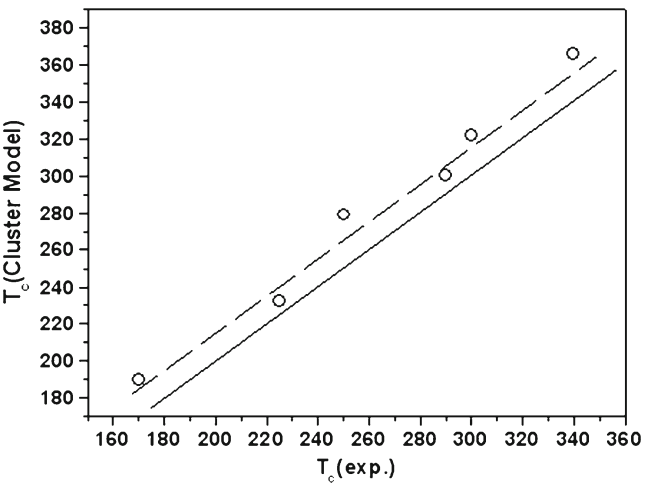

Fig. 5 Comparison between the experimental Curie temperature T_c (in kelvin) and the theoretical Curie temperatures determined by the cluster expansion method from the data in Table 2. The *dashed line* displays a consistent overshoot of roughly 15 K relative to the *solid line* representing perfect theory-experiment agreement

covering the entire series, including MnFeAs, that relates T_c to the fractional expansions,

$$T_c(x) = 280\Big(1 + 22.3\ \ \delta a(x)\Big/a_0 - 21.9\ \ \delta c(x)\Big/c_0\Big) = 280 f(x) \quad (29)$$

with $c_0 = c(x=0.50) = 0.3486$ nm and $\delta c = c(x) - c_0$.

Motivated by the accurate calculation of T_c for MnFeAs, we now combine Eq. (29) with cluster method calculations to gather novel information. To this end, we will adopt a hypothesis often found in the literature [1–3, 21, 22] and assume that the compositional dependence of the exchange constants $J_{11} \ldots J_{22}$ and K for $MnFeAs_xP_{1-x}$ follows that of the Curie temperature, that is, is given by the function $f(x)$ defined by Eq. (29). We divide the exchange constants in Table 1 by $f(x=1) = 0.671$ to obtain the constants for the composition $x=0.50$ and then multiply the latter by $f(x)$ to find the coupling constants for the other compounds in the series. Table 2 displays the resulting exchange constants for all the compositions in [17]. Figure 4 displays the logarithmic plots of Δ as a function of the temperature for each set of parameters in Table 2. As in Fig. 2, a cusp identifies the cluster method Curie temperatures for each composition.

Figure 5 plots the experimental Curie temperature as a function of the theoretical T_c. The deviations amount to roughly 5 %, the calculated temperatures systematically overshooting the measured T_c by about 15 K. The overshoot seems to be a characteristic of the cluster methods: For simple lattices, the predicted T_c overestimate the HTE results [4, 5]. We could therefore have expected the Curie temperatures in Fig. 4 to exceed the experimental values. Other simplifications in our model are expected to contribute to the disagreement between theory and experiment. More accurate predictions might have been made, for instance, if the interaction with more distant neighbors along the c-axis were considered, and no attention has been given to the expected itinerancy of at least a fraction of the electrons.

The observed transitions in the studied series are discontinuous and usually regarded as of first order. The discontinuity can be traced back to an important magneto-elastic effect not considered in our model, which therefore predicts continuous or second-order transitions. Had the samples been clamped in the laboratory, their deformation would be restrained, the measured T_c would be a few degrees lower, and larger deviations from the theoretical values would result.

Finally, we point out that direct inspection of Eqs. (24)–(27) would have allowed to foresee the close agreement with experiment in Fig. 5, given that the linear extrapolation method used to determine the coupling constants is derived from the compositional dependence of T_c. The procedure based on Eq. (29) transfers the accuracy obtained for MnFeAs to the other compositions. It must be stressed that the method should therefore be put to additional test via derivation of thermo-magnetic properties from the coupling constants in Table 2 and comparison with experiments.

4 Conclusions

We have carried out a detailed analysis of experimental data on MnFeAs and $MnFeAs_xP_{1-x}$ ($0.25 \le x \le 0.65$). Exchange coupling constants, crystallographic data, and magnetization measurements have been combined in a unified analysis [12, 13, 16, 17]. One objective of the present work was to construct a model for the magnetic moment interactions in these compounds more accurate than that resulting from plain MFT [1–3]. For this purpose, Callen's cluster expansion method [10, 11] was adopted to analyze the interactions in the spin system. On the basis of the data in [12], the cluster method yielded an accurate estimate of the Curie temperature for hexagonal MnFeAs. Extrapolation of the data in [12] to the range of compositions of interest for magnetocaloric applications yielded exchange couplings that pave the road to the calculation of thermo-magnetic properties. Care was taken in the construction of that extrapolation to insure simultaneous consistency with the measured T_c for all compositions tested, within 5 % accuracy, and with the expected variation of such constants with lattice expansion in both the a and c directions. The results confirm that strong intra-plane Mn–Mn and inter-plane Mn–Fe couplings are essential to obtain room-temperature T_c's in this class of compounds, while intra-plane Fe–Fe interactions were shown to be less important. Additional work is under way to calculate thermo-magnetic properties from the coupling constants in Table 2 via cluster expansion. Comparison with the available experimental data will provide a definitive test of the accuracy afforded by our approach.

References

1. N.A. de Oliveira, P.J. von Ranke, Phys. Rpts. **489**, 89 (2010)
2. P.J. von Ranke, A. de Campos, L. Caron, A.A. Coelho, S. Gama, N.A. de Oliveira, Phys. Rev. **B70**, 094410 (2004)
3. P.J. von Ranke, N.A. de Oliveira, B.P. Alho, V.S.R. de Sousa, E.J.R. Plaza, A.M.G. Carvalho, J. Magn. Magn. Mater. **322**, 84 (2010)
4. J.S. Smart, *Effective field theories of magnetism* and references therein (Saunders, Philadelphia, 1966)
5. G.S. Rushbrooke, P.J. Wood, Mol. Phys. **1**, 257 (1958)
6. M.B. Stearns, Phys. Today, p.34, April issue (1978)
7. R. Mota, M.D. Coutinho Filho, Phys. Rev. B **33**(7724) (1986)
8. V.P. Antropov, M.I. Katsnelson, B.N. Harmon, M. van Schilfgaarde, D. Kusnezov, Phys. Rev. B **54**, 1019 (1996)
9. J.J. Pulikkotil, I. Ke, M. van Schilfgaarde, T. Kotani, V.P. Antropov, Supercond. Sci. Technol. **23**, 054012 (2010)
10. B. Strieb, H.B. Callen, G. Horowitz, Phys. Rev. **130**, 1798 (1963)
11. H.B. Callen, E. Callen, Phys. Rev. **136**, A1675 (1964)

12. X.B. Liu, Z. Altounian, Their coupling parameters include a factor of 2 (X. Liu, private comm.). J. Magn. Magn. Mater. **321**, 2005 (2009)
13. J. Tobola, M. Bacmann, D. Fruchart, P. Wolfers, S. Kaprzyk, A. Kounina, J. Alloys Compd. **317–318**, 274 (2001)
14. E. Brück, O. Tegus, D.T. Cam Thanh, Nguyen, T. Trung, K.H.J. Buschow, Int. J. Refrig. **31**, 763 (2008)
15. E. Brück, M. Ilyn, A.M. Tishin, O. Tegus, J. Magn. Magn. Mater. **290–291**, 8 (2005)
16. M. Bacmann, J. Soubeyroux, R. Barrett, D. Fruchart, R. Zach, S. Niziol, R. Fruchart, J. Magn, Magn. Mater. **134**, 59 (1994)
17. O. Tegus, E. Brück, L. Zhang, W. Dagula, K. Buschow, F.R. de Boer, Physica **B319**, 174 (2002)
18. H.A. Brown, Phys. Rev. **B4**, 115 (1971)
19. E. Merzbacher, *Quantum mechanics*, 2nd edn. (Wiley, New York, 1970). ch. 17
20. G.G. Cabrera, Am. J. Phys. **46**, 1062 (1978)
21. D.S. Rodbell, J. Owen, J. Appl. Phys. **35**, 1002 (1964)
22. C.P. Bean, D.S. Rodbell, Phys. Rev. **126**, 104 (1962)